COMPARATIVE SAFETY PHYSICS PARAMETERS IN THE ADVANCED FUELS CRITICAL ASSEMBLIES

S. K. Bhattacharyya, D. C. Wade, R. G. Bucher
W. R. Robinson, and R. W. Schaefer
Argonne National Laboratory
Argonne, Illinois U.S.A.

ABSTRACT

The interest in the use of advanced fuels (carbide and advanced oxide) in LMFBR's stems from the projected improvement in breeding properties over conventional mixed-oxide fuels. This improvement in breeding is a consequence of the higher fuel volume fractions achievable in the advanced fuels designs and the concomitant harder neutron spectrum and lower enrichment. The impact of these changes, not only on the breeding properties but also on the safety physics parameters (^{238}U Doppler effect, sodium void effect, and ^{10}B control rod worth), has a strong bearing on whether these fuels are ultimately adopted. A set of key integral physics parameters were measured in a series of advanced fuels critical assemblies constructed on ZPR-9 to assess the relative safety and breeding properties of candidate advanced fuels. The experimental results confirmed the projected improvement in the breeding properties in advanced fuels cores relative to current oxide LMFBR cores, and revealed that the accompanying changes in the safety-related physics parameters were generally large and of unfavorable sign. Specifically, it was found that relative to the ZPR-6, assembly 7 benchmark "current mixed-oxide" values for normalized parameters, the central ^{238}U Doppler worth decreased by 20-40%, the central ^{10}B worth decreased by 10 to 20% and the central (non-leakage component) sodium void reactivity worth increased by 30 to 40% in the advanced fuels compositions. It was shown that the C/E values on safety parameters in the advanced fuels compositions are of comparable size to those in current oxide assemblies.

INTRODUCTION

A series of critical experiments have been performed on the ZPR-9 facility at Argonne National Laboratory to study the relative neutronic properties of advanced fast reactor fuels. The program of measurements was designed to provide a basis for evaluating both the analysis techniques and basic nuclear data used in advanced fuels breeder designs. In this paper, results of the measurements of the safety physics parameters in these advanced fuels assemblies are reported along with calculated

predictions using standard methods. The results have been compared to corresponding values in "current-oxide" compositions, which have previously been studied at length in critical facilities.

The experiments were conducted on three related critical assemblies: the Carbide Benchmark, the Carbide Zone, and the Advanced Oxide Zone assemblies. The unit cell compositions for these assemblies were referenced to advanced fuels breeder designs in the 1200 MWe range. The Carbide design was provided by Barthold et al,[1] (ANL) while the advanced oxide design was provided by Cowan[2] (General Electric). To within the constraints imposed by the presence of the ZPR matrix and available materials inventory, the carbide benchmark core composition matches the fuel characteristics of the outer core zone of the 1200 MWe carbide design, while the carbide zone matches the inner core zone of the same design. The advanced oxide zone matches the core-average fuel properties of the 1200 MWe advanced oxide design. The matching of compositions was not exact because of the aforementioned constraints and the desirability of having a simple, easily analyzable unit cell. Table 1 displays the ratios of the atom concentrations achieved in the critical assemblies to the target, 1200 MWe-design atom concentrations.

TABLE 1. Comparison of Advanced Fuels Assembly Physical Characteristics with Target Design Parameters

Parameter	Ratio of Carbide Benchmark to ANL Carbide Outer Core[a] Value	Ratio of Carbide Zone to ANL Carbide Inner Core[a] Value	Ratio of Oxide Zone to GE[b] Advanced Oxide Value (average of inner and outer core)
Fissile Atom Density	0.96	0.91	0.98
Heavy Metal (HM) Density	0.97	0.92	1.01
Enrichment (Fissile/HM)	0.98	0.98	0.96
U-238/Pu-239 Atom Ratio	0.93	0.94	0.96
C or O/HM Atom Ratio (as appropriate)	0.95	1.20	1.01
NA/HM Atom Ratio	0.88	0.95	0.72
FE/HM Atom Ratio	1.34	1.30	1.39
Fuel (U+Pu+C or O) Vol. Frac.	1.00	1.05	1.13
Coolant Vol. Frac.	0.79	0.79	0.67
Structure Vol. Frac.[c]	1.71	1.57	1.45

[a] ANL 1200 MWe Carbide Design (.375 in. pin) Na Bonded, beginning-of-life composition.

[b] GE 1200 MWe Advanced Oxide Design, beginning-of-equilibrium cycle composition.

[c] Includes void fraction.

Relative to the "current-oxide" designs, a major feature of the "advanced fuel" designs is a high fuel volume fraction obtained at the expense of structure, and a resultant higher fertile/fissile atom ratio (lower enrichment). This is indicated in Table 2 where several central core properties of the advanced fuels compositions are compared with each other and with the "current-oxide" ZPR-6 assembly 7 (ZPR6/7) and GCFR reference assembly (GCFR-II) compositions. The very much higher heavy metal density in the advanced fuels cores results in a harder spectrum in these cores relative to the "current oxide" LMFBR cores. Calculated

spectra are intercompared in Figs. 1 and 2; Figs. 3 and 4 display calculated adjoint spectra. The spectral hardening indicated in the figures has been confirmed experimentally by measured reaction rate ratios. The physics properties of the advanced fuels compositions are governed by the hardened spectrum.

TABLE 2. Primary Characteristics of the Advanced Fuels and Reference LMFBR and GCFR Cores

Parameter	Benchmark	Carbide Zone	Oxide Zone	GCFR-II	ZPR6/7 (Current Oxide)
Fissile Atom Density	1.382 + 21	0.933 + 21	0.930 + 21	1.221 + 21	0.916 + 21
Heavy Metal (HM) Density	11.377 + 21	10.825 + 21	9.264 + 21	6.923 + 21	6.812 + 21
Enrichment (Fissile/HM)	0.121	0.086	0.100	0.176	0.134
$^{238}U/^{239}Pu$ Atom Densities	7.38	10.93	9.18	4.68	6.52
C/HM or O/HM Densities	0.95	1.20	1.99	1.94	2.05
NA/HM Atom Densities	0.80	0.86	0.73	0.00	1.36
FE/HM Atom Densities	0.90	0.87	1.22	2.21	1.90
Fuel (U+Pu+C or O) Vol. Frac.	0.38	0.40	~0.43	0.26	0.33
Coolant Vol. Frac.	0.38	0.38	0.28	0.42	0.42
Structure + Void Vol. Frac.	0.24	0.22	~0.29	0.32	0.25
Zero Excess Critical Mass (kg)*	534.1	599.5	573.9	1107.5	588.8
k_∞	1.3188	1.0816	1.1150	1.4874	~1.25
$\overline{r^2}$ (cm^2)++	1086	1157	1211	3000	~1600

*The uncertainties on these masses are of the order of 1%.
++Mean-squared distance traveled from neutron birth to fission event.

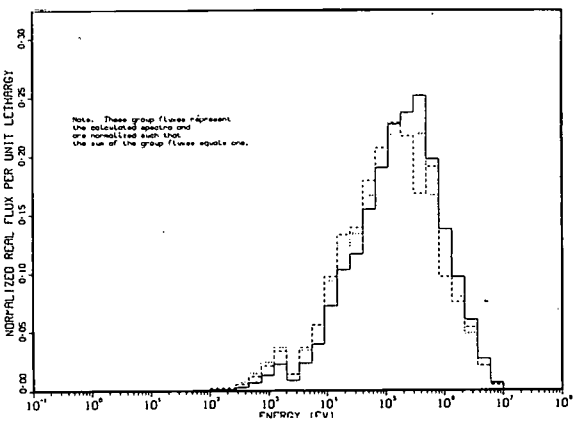

Fig. 1. Calculated central real spectra in advanced fuels assemblies. (Carbide benchmark-solid line; carbide zone-dotted line; oxide zone-dashed line).

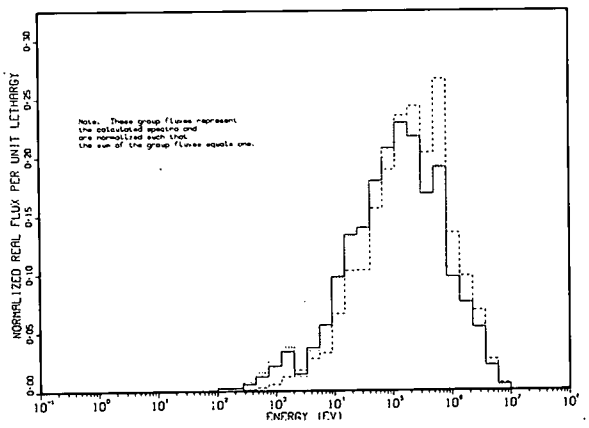

Fig. 2. Calculated central real spectra in oxide fueled LMFBR assemblies, (Advanced oxide zone-solid line, ZPR6-7-dotted line, GCFR-II--dashed line).

Figure 5 shows a sketch of the carbide benchmark assembly, giving the principal radial and axial dimensions. The assembly had a simple, uniform core composition. The other two assemblies used the benchmark as a framework to contain a central zone of an advanced fuels composition. Both

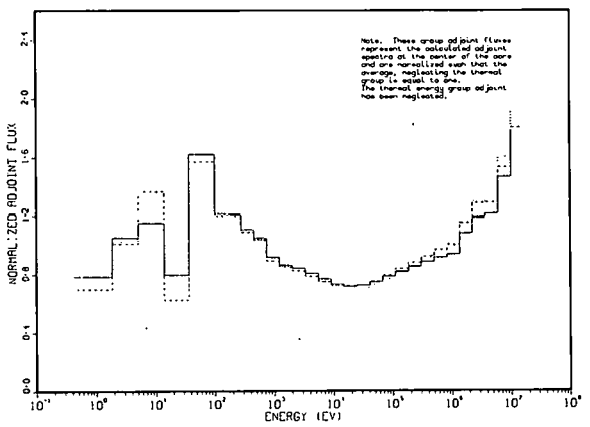

Fig. 3. Calculated central adjoint spectra in advanced fuels assemblies. (Carbide benchmark-solid line; carbide zone-dotted line; oxide zone-dashed line).

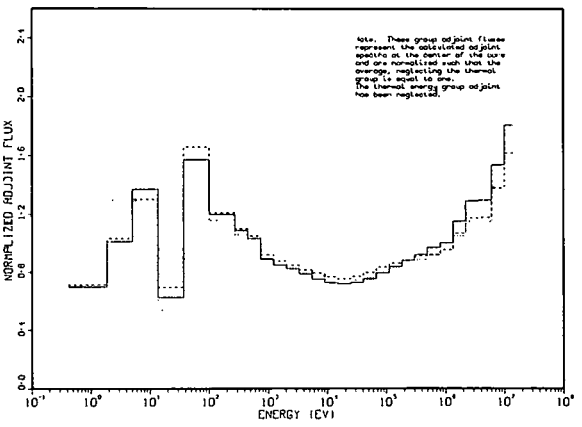

Fig. 4. Calculated central adjoint spectra in oxide fueled LMFBR assemblies. (Advanced oxide zone-solid line; ZPR6/7-dotted line; GCFR-II--dashed line).

the carbide and advanced oxide zones had a zone radius of 31.32 cm. The use of zones was adequate since spectral rather than spatial aspects of advanced fuels designs were being investigated.

For the zone size selected, spectral indices from a fundamental mode, fine-group SDX[3] calculation agreed very well with core center-values produced with broad group RZ diffusion theory calculations of the zoned assemblies. This established the fact that the zone sizes were sufficiently large to ensure that the central spectra were characteristic of the zone composition, uncontaminated by spectral transients propagating into the zones from the driver region. The blanket and reflector for the carbide zone assembly was the same as that for the benchmark. This was also true of the advanced oxide zone assembly except that there was an oxide axial blanket above the oxide zone.

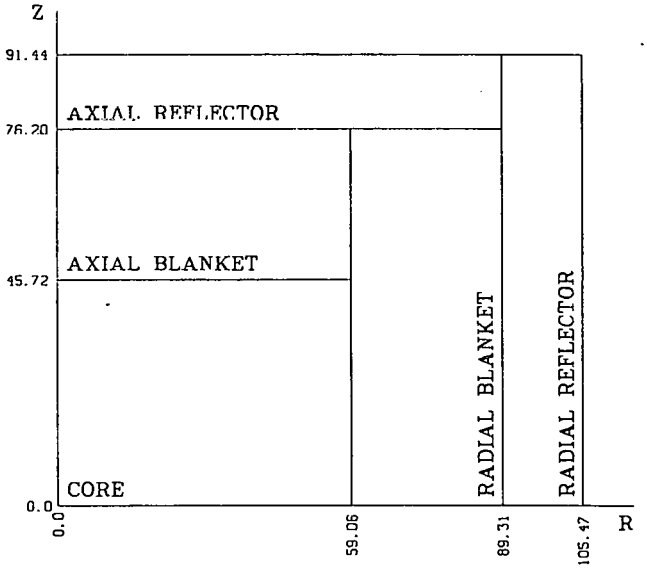

Fig. 5. Schematic sketch of the carbide benchmark assembly giving radial and axial dimensions.

SAFETY PHYSICS PARAMETERS MEASURED

The following safety physics parameters were measured in the Advanced Fuels Critical Assemblies.

a. Small sample reactivity worths of ^{239}Pu, ^{238}U, ^{10}B, Na, stainless steel.
b. ^{238}U Central Doppler reactivity worths.
c. B_4C control rod worths.
d. Sodium void worths.

EXPERIMENTAL AND CALCULATIONAL METHODS

The small sample reactivity worths and the ^{238}U central Doppler worth were measured using the sample oscillation reactivity-difference technique. The large reactivity changes involving sodium void and B_4C control rod worths were determined as the differences of the subcriticalities of two reactor configurations.

Analyses of the experiments were performed with ENDF/B-IV nuclear data and two-dimensional diffusion theory methods in a 29 broad group energy structure. Unit cell averaged isotopic cross-sections were generated for all appropriate compositions using the MC^2-2[4]/SDX[3] codes wherein spatial heterogeneity effects were explicitly taken into account. Anisotropic diffusion coefficients were used to account for direction-dependent neutron transport within the diffusion theory framework. The Gelbard method[5] was used to generate these anisotropic diffusion coefficients in core regions for neutron energies exceeding 2 keV; for all other cases the Benoist method[6] was used. These coefficients were input as multipliers applied to the isotropic diffusion coefficients, $1/3\ \Sigma_{tr}$.

EXPERIMENTAL RESULTS AND COMPARSION WITH CALCULATIONS

Small Sample Reactivity Worths

The central small sample reactivity worths of a number of materials of interest were measured in the three assemblies. These worths, along with associated measurements of reactivity worth spatial distributions are useful for material redistribution worth calculations in accident analyses. The results of the measurements are displayed in Table 3, along with values for the "current-oxide" (LMFBR and GCFR) reference assemblies.[7,8] The worths are normalized to the central worth of ^{239}Pu to enable a comparison of the worths independent of the effects of changed perturbation denominator between the assemblies. The normalized worths follow a predictable trend given the relative hardness of the spectra in the different assemblies (Figs. 1,2) and the corresponding adjoint

spectral shapes (Figs. 3,4). Relative to the ZPR6/7 value, the normalized ^{238}U worth is 22% smaller in the carbide benchmark, and 29% smaller in the GCFR-II. The ^{10}B worth is 20% smaller in the carbide benchmark and in GCFR-II.

The worths were calculated using first order perturbation theory methods, and the resulting C/E (calculated/experimental) ratios are shown in Table 3. The central worth of ^{239}Pu is predicted slightly better in the carbide and advanced oxide zones than in the other three assemblies. The chronic problem with the prediction of light scatterer worths is clearly seen in Table 3. The normalized ^{238}U and ^{10}B worths are predicted relatively consistently in the assemblies. The trend of increasing underprediction of the ^{10}B worth with increasing hardness of the spectrum has been attributed[9] to an increasing underprediction of the low energy flux for harder spectrum assemblies.

TABLE 3. Small Sample Central Reactivity Worths in the Various Assemblies

	Carbide Benchmark		Carbide Zone		Oxide Zone		GCFR Phase II		ZPR6/7	
Isotope	Experimental Worth (Ih/kg) or ratio	C/E	Experimental Worth (Ih/kg) or ratio	C/E	Experimental Worth (Ih/kg) or ratio	C/E	Experimental Worth (Ih/kg) or ratio	C/E	Experimental Worth (Ih/kg) or ratio	C/E
^{239}Pu	268.7 ± 2.8	1.19	159.1 ± 2.7	1.13	178.1 ± 1.7	1.13	231.4 ± 2.6	1.19	158.3 ± 2.1	1.19
Worth Ratios										
$^{238}U/^{239}Pu$	-0.054 ± 0.002	0.88	-0.059 ± 0.002	0.90	-0.055± 0.002	0.98	-0.049 ± 0.002	0.93	-0.069 ± 0.003	0.87
$^{10}B/^{239}Pu$	-14.84 ± 0.29	0.87	-16.74 ± 0.39	0.90	-16.91 ± 0.31	0.88	-14.81 ± 0.28	0.83	-18.61 ± 0.44	0.94
$Na/^{239}Pu$	-0.056 ± 0.004	1.19	-0.054 ± 0.004	1.08	-0.045± 0.003	1.32	---		---	
Stainless Steel/^{239}Pu	-0.034 ± 0.001	1.22	-0.033 ± 0.001	1.18	-0.033± 0.001	1.14	-0.033 ± 0.001	1.17	---	
Ih/%Δk/k conversion ratio (calculated)	922.4		916.7		920.0		944.3		974.8	

Central ^{238}U Doppler Effect

The Doppler reactivity worth of a small (~1.1 kg) UO_2 sample was determined at the center of the three assemblies as a function of temperature for the range 300°K to 1100°K. The ^{238}U Doppler worths extracted from these measurements are shown in Fig. 6 for the three cases. The curves represent least squares fits to the experimental data (corrected for empty capsule Doppler effects) to an expression of the form

$$\rho(T) = \frac{C_1 T_o}{1-\gamma}\left[\left(T_1/T_o\right)^{1-\gamma}-1\right] + C_2 \qquad (1)$$

where T_o is the reference temperature, C_1, C_2 and γ are the fitting paramters and $\rho(T)$ is the reactivity as a function of temperature in °K. The figure shows that the measured ^{238}U Doppler worth was largest for the carbide benchmark assembly and smallest for the carbide zone (for a temperature range of 300°K to 1100°K the carbide zone value was 25.4% smaller than that in the benchmark).

Table 4 lists the values of the ^{238}U Doppler worths normalized to the central ^{239}Pu worths in the same assembly for the three cases

with corresponding values for ZPR-6/7 and GCFR-II. The normalized worths in the carbide and advanced oxide zones are similar, the advanced oxide zone value being 7.34% larger. The carbide benchmark core value is considerably smaller, attesting to the fact that the spectrum in this assembly was the hardest. The normalized ^{238}U Doppler worths in the advanced fuels assemblies are intermediate between the values in the LMFBR and GCFR benchmark assemblies, as would be expected from relative spectrum hardness considerations. Relative to the "current"/mixed oxide LMFBR case, the advanced fuels cores show a 19-41% reduction in the normalized ^{238}U Doppler worth, whereas the corresponding reduction in the GCFR benchmark value was 54%.

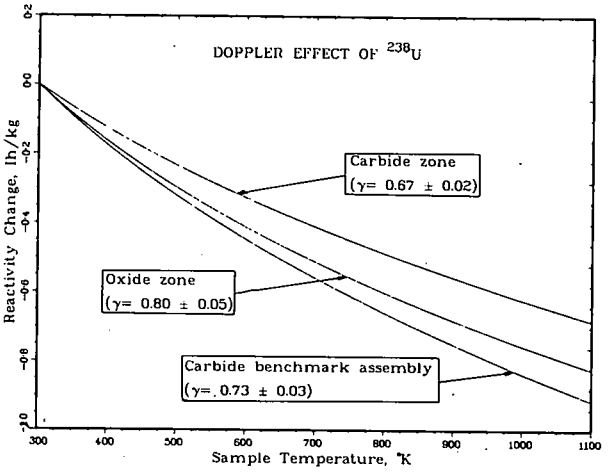

Fig. 6. Central ^{238}U Doppler worth as a function of temperature for the three advanced fuels critical assemblies.

The Doppler reactivity effect was calculated using a modified first order perturbation theory method[9] in which the flux perturbation effect of the sample and the hot sample/cold core resonance interaction effect were taken into account. For the ZPR-6 assembly 7 case ENDF/B-I data were used; for the other cases ENDF/B-IV data were used. The C/E values for the normalized ^{238}U Doppler worth for all the assemblies are listed in Table 4. The primary C/E discrepancy in Table 4 is the relatively large overprediction of the carbide zone ^{238}U Doppler worth. This has been attributed to an overprediction of the low energy component of the real spectrum in the carbide zone. The reason for this overprediction of the low energy spectra is not fully understood at this time. The effects of variations in the sodium resonance scattering cross-section and iron elastic scattering cross-section are being investigated.

TABLE 4. Comparison of Normalized ^{238}U Doppler Worths for the Advanced Fuels Critical Assemblies and Typical LMFBR and GCFR Critical Assemblies

Assembly	^{238}U Doppler Effect Ih/kg (~±0.01)	^{239}Pu Central Reactivity Worth Ih/kg (~±1.0)	$\frac{^{238}U \text{ Doppler}}{^{239}Pu \text{ Worth}}$ (Units of 10^{-3})	% Change Relative to Reference Oxide LMFBR	Calculated Predictions: C/E of ^{238}U Doppler Effect	Calculated Predictions: C/E of Normalization ^{238}U Doppler Effect
Carbide Benchmark	-0.915	209	+3.41	-40.35	0.874	0.734
Carbide Zone	-0.683	155	+4.29	-24.96	1.027	0.909
Advanced Oxide Zone	-0.824	172	+4.63	-19.01	0.880	0.778
ZPR-6 Assy 7 Current Oxide LMFBR	-0.905	156	+5.81	0	1.030*	0.761*
GCFR Phase II Assembly	-0.623	231	+2.69	-53.7	0.827	0.713

*ENDF/B-I cross-sections. All other cases used ENDF/B-IV cross-sections.

B_4C Control Rod Worths

An indication of the relative worths of B_4C control rods in the three advanced fuels assemblies and in GCFR-II relative to ZPR6/7 may be inferred from the measured small sample central worths of ^{10}B. From Table 3 it is seen that relative to ZPR6/7, the worth of ^{10}B decreases by 20% in the carbide benchmark and GCFR-II cores and by approximately 10% in each of the advanced fuels zones. This sets an upper bound on the decreased worths of control rods that might be expected in the advanced fuels systems.

The worth of a simulated B_4C control rod was measured at the center of the carbide benchmark core. The worth was determined relative to a sodium-filled control rod position reference. The simulated rod extended through the axial height of the core (±18 inches). A corresponding measurement had been performed in ZPR6/7.[12] For the carbide benchmark, the simulated rod had a higher B_4C concentration (^{10}B atom concentration of 7.17×10^{21} atoms/cm^3) than for ZPR6/7 (^{10}B atom concentration of 3.80×10^{21} atom/cm^3). The measured worth of the simulated rod in the carbide benchmark was 755.9 ± 4 Ih, which was 79% greater than the corresponding value of 421.6 ± 19.1 Ih in ZPR6/7. On a per unit ^{10}B atom concentration basis, the control rod worth in the carbide benchmark was 5% less than that in ZPR6/7. Unfortunately, a direct comparison between the two is not possible because of the different core heights in the two cases.

Using eigenvalue difference techniques and infinitely dilute ^{10}B isotopic cross-sections, a C/E value of 0.978 was obtained for the control rod worth relative to a sodium filled control rod channel in the carbide benchmark. This is slightly lower than past experience (C/E values of 1.01 to 1.05 are typical on current oxide assemblies.)

Sodium Void Worth Measurement

The reactivity worths of voiding sodium in small central zones were measured in the advanced fuels assemblies and in ZPR6/7[10] by the rod-drop subcriticality technique. For the advanced fuels assemblies the sodium voided zone was 5 × 5 drawers square (equivalent radius 15.58 cm) and for ZPR6/7 the zone size was 3 × 3 drawers square (equivalent radius 9.35 cm). The heights of the sodium voided zones for the advanced fuels assemblies and ZPR6/7 were not the same, and it is meaningful to discuss the central values and the full core height values of the sodium void worth separately.

Central (non-leakage) sodium void worth component

For the advanced fuels assemblies a measurement was made for an axial extent of ±5 inches from the midplane; for ZPR6/7 a measurement was made for an axial extent of ±6 inches from the midplane. The sodium void worths from these measurements, suitably normalized to unit sodium weights and to the central ^{239}Pu worth, are shown in Table 5. These numbers can be compared directly, and it is seen that the advanced fuels

TABLE 5. Central Sodium Void Worths in the Advanced Fuels and Reference Oxide Assemblies

Parameter	Carbide Benchmark	Carbide Zone	Advanced Oxide Zone	Current Oxide (ZPR6/7)
Central Sodium Void Worth (Ih/kg)	+15.1 ± 0.2	9.78 ± 0.2	10.7 ± 0.3	6.94 ± 0.6[a]
Normalized Central Sodium Void Worth (Ih/kg)/(^{239}Pu Ih.kg) · 10^2	5.620	6.148	6.009	4.384
Change from ZPR6/7 (%)	+28.2	+40.2	+37.1	---

[a]This measurement was made for a 3 × 3 drawer central zone 12 in. high. The advanced fuels assembly measurements were made for a 5 × 5 drawer central zone 10 in. high.

compositions display a 30 to 40% more positive central normalized sodium void coefficient than does ZPR6/7. This comparison of the non-leakage component of the sodium void worth is a function both of the flux spectrum and of the slope versus energy of the adjoint (which is made steeper by lower enrichment). The relative values of the worths are compatible with the relative spectral shapes shown in Figs. 1-4.

The central sodium void worth was calculated for the carbide benchmark case using an eigenvalue difference technique. The isotopic cross-sections and anisotropic diffusion coefficients were regenerated for the sodium voided composition. A C/E value of 1.067 was obtained. This is somewhat less than the ratios obtained for earlier current oxide sodium-void experiments.[11]

Full core height sodium void worths

For each of the cores in the advanced fuels program, the central 5 × 5 drawer region was voided in four axially-symmetric voiding steps (±0-5 in., ±5 to 11 in, ±11 to 18 in., and--in the blanket--±18 to 30 in.) leading to a full core-plus-axial-blanket voided 5 × 5 drawer central zone. Only the carbide benchmark measurements were calculated. Eigenvalue difference calculations were made both of the individual voiding steps and of the cumulative void worth. Both cross sections and anisotropic diffusion coefficients were regenerated specifically for the sodium-voided unit cells. For the carbide benchmark, the incremental and cumulative specific sodium void worths and the associated C/E values were:

Axial increment	Experimental Ih/kg Na	C/E Gelbard D's	C/E Gelbard D in core Benoist D in Blk	C/E Gelbard D in core $1/3\Sigma_{tr}$ in Blk
±0-5"	+16.114	1.067		
±5-11"	+7.783	1.12		
±11-18"	-7.313	1.02		
total core	+3.69	1.12		
±18-30" blk	-3.88	1.85	1.11	0.62
core+blk	+0.71	-0.44	1.12	2.32

In the core, both the leakage and nonleakage components are accurately calculated if streaming is accounted for using Gelbard anisotropic

diffusion coefficients. The Gelbard D's fail in the blanket (their derivation rests on the existance of a well-defined positive buckling); but it is seen that for this case Benoist D's produce accurate blanket results.

A direct comparison of the full core height sodium void worths between the advanced fuels measurements and ZPR6/7 is inappropriate because of the different core heights of the assemblies. However, the C/E values obtained for the carbide benchmark advanced fuels composition are comparable with the extensive experience on current oxide compositions reported by Beck et al."

CONCLUSIONS

An indicator of the breeding properties of an assembly is the instantaneous core point conversion ratio, which is defined (to within 2%) as,

$$CR_p = \frac{28_N}{49_N} \quad \frac{28_c}{49_f(1+49_{\bar{\alpha}})} \qquad (2)$$

The ratio of the atom concentration gives the effect of enrichment on the conversion ratio, while the other term gives a spectral effect. The terms in the spectral component are measurable. Table 6 summarizes the experimental evidence for the improved breeding properties of the advanced fuels

TABLE 6. Summary of Improved Conversion Ratios in Advanced Fuels Assemblies

Parameter		Carbide Benchmark	Carbide Zone	Oxide Zone	ZPR6/7	GCFR-II
Compositions						
Fuel Vol. Frac.	(%)	38	40	43	33	26
Enrichment	(a/o)	12.1	8.6	10.0	13.4	17.6
N^{28}/N^{49}	(atom ratio)	7.38	10.93	9.18	6.52[a]	4.68
K_∞		1.319	1.082	1.115	~1.25	1.487
$\overline{\ell^2}$	(cm^2)	1086	1157	1211	~1600	3000
Spectral Indicators (Cell Average Reaction Rates)						
c^{28}/f^{49}	(±~1.5%)	0.1230	0.1367	0.1387	0.1396[a]	0.1196
f^{28}/f^{49}	(±~2%)	0.0252	0.0208	0.0225	0.0242	0.0330
Core Conversion Properties						
$\frac{c^{28}}{f^{49}(1+\alpha^{49})}$	(±~3.8%)	0.0983	0.1026	0.1081	0.1087[a]	0.0990
$CR = \frac{N^{28}}{N^{49}} \frac{c^{28}}{f^{49}(1+\alpha^{49})}$		0.726	1.122	0.992	0.715[a]	0.464[b]
Deviation from current oxide %		+1.54	+56.92	+38.74	---	-35.10

[a] Since conversion ratio measurement was not made in ZPR6/7, the conversion ratio reported here was measured in ZPPR4 Assembly 1 inner core at location 137-34. The unit cell composition in this assembly was identical to that in ZPR6/7. The N^{28}/N^{49} ratio was 6.58 in ZPPR4/1 (i.e., 1% greater than in ZPR6/7) while the c^{28}/f^{49} value was 0.1443 (3.3% greater than in ZPR6/7).

[b] Because of the large amount of leakage from GCFR cores, the core point conversion ratio is not a good indicator of total breeding properties. A significant fraction of the total breeding occurs in the radial and axial blankets. The core point conversion ratio for GCFR II is included here only for completeness. The computed breeding ratio for the current GCFR designs is ~1.4.

assemblies and the background information necessary for its interpretation. The experimental conversion ratio and spectral index data have been obtained from Bretscher and Morman.[13]

The heavy metal volume fraction is larger in the advanced fuels case than for ZPR6/7. This causes spectrum hardening and thus a reduction of parasitic capture. As a consequence, the enrichment can be reduced (i.e., N^{28}/N^{29} can be increased) in the advanced fuels cores. The fact that the spectra in the advanced fuels cores are harder is seen from the spectral indices. It is seen from the table that the spectral component of the conversion ratio actually decreases with harder spectra. The c^8/f^9 ratio and $(1+\alpha^{49})$ value both decrease with increasing spectrum hardness, and the net effect is a balance between the two opposing effects. However the much increased N^{28}/N^{29} ratio in the advanced fuels assemblies causes the net conversion ratio to increase relative to the current-oxide value. For the carbide benchmark case, the increase is nominal (1.5%), but for the carbide and advanced oxide zone the increase is dramatic (57 and 39% respectively). This analysis also makes evident the fact that the enrichment reduction has the dominant effect on the conversion ratio while the spectral effect is small. In a GCFR the core point conversion ratio is decreased both by the harder spectrum and by the decreased N^8/N^9 ratio necessitated by the large leakage for the core. The blanket conversion ratios are very high, however, and the net effect is a high breeding ratio.

Associated with the improvement in the breeding properties shown in Table 6, is a penalty in the safety properties. In Table 7, the experimental evidence for the change in values of the safety coefficients is listed. It is seen that the changes are significantly large and of an unfavorable sign in all cases. Additionally, the results in Tables 3-5 (and in the text for sodium void and control rod worths) establish that the C/E values for parameters in advanced fuels compositions are not significantly different than for the current oxide composition.

TABLE 7. Summary of the Safety Related Physics Properties of Advanced Fuels Cores

Safety Physics Parameter	Significance	% Change from Current Oxide LMFBR Value			
		Carbide Benchmark	Carbide Zone	Oxide Zone	GCFR-II
ρ^{B-10}/ρ^{49}	Indicator of Control Rod and Poison Worths	-20.3	-10.0	-9.1	-20.4
$\rho^{\text{Doppler } 28}/\rho^{49}$ (ΔT 300-1100°K)	Primary inherent Safety Coefficient	-40.4	-25.0	-19.0	-53.7
$\rho^{\text{Central Na Void}}/\rho^{49}$	Spectral component of sodium void coefficient	+28.2	+40.2	+37.1	---

In summary, the comparative safety physics parameters of advanced fuels systems have been determined experimentally. It was found that relative to current oxide LMFBR's, the improved breeding properties were accompanied by significant degradation of safety coefficients. Safety performance is governed not only by the safety coefficients but by design

loadings as well. Thus, an equally important fact is that the biases in the calculated predictions of the safety coefficient were shown to not change significantly from those in the current-oxide LMFBR system. The results presented in this paper provide the designer with quantitative information on which to base advanced fuels LMFBR designs for optimum breeding and safety performance.

REFERENCES

1. W. P. Barthold et al., Personal Communication, Argonne National Laboratory, 1976.
2. C. L. Cowan, Personal Communication, General Electric Company, 1976.
3. W. M. Stacey et al., "A New Space-Dependent Fast Neutron Multigroup Cross-Section Preparation Capability," Trans. Am. Nucl. Soc., 15, 292 (1972).
4. H. Henryson II, B. J. Toppel and C. G. Stenberg, "MC^2-2: A Code to Calculate Fast Neutron Spectra and Multigroup Cross-Sections," ANL-8144, Argonne National Laboratory, (1976).
5. E. M. Gelbard et al., "Calculations of Void Streaming in the Argonne Gas Cooled Fast Reactor Critical Experiments," Nucl. Sci. Eng., 64 (2) 624 (1977).
6. P. Benoist, "Streaming Effects and Collision Probabilities in Lattices," Nucl. Sci. Eng., 34, 285 (1968).
7. R. D. McKnight, "Benchmark Testing Using ENDF/B-III and IV" Nucl. Sci. Eng., 62, 309 (1977).
8. R. B. Pond, editor, "Reactor Physics Studies in the GCFR Phase-II Critical Assembly," ANL-76-108, Argonne National Laboratory (1976).
9. S. K. Bhattacharyya and R. B. Pond, "Measurement of the ^{238}U Doppler Effect in GCFR Critical Assemblies," Nucl. Sci. Eng., 65, 548 (1978).
10. L. G. LeSage et al., "Sodium Void and Small-Sample Reactivity Worth Measurements in ZPR-6 Assembly 7," ANL-7910, pp. 141-154, Argonne National Laboratory (1972).
11. C. L. Beck et al., "On the Extrapolation of ZPR Sodium Void Measurements to the Power Reactor," Proc. International Meeting on Fast Reactor Safety and Related Physics, CONF 761001, Vol. II, pp. 512-520, (1976).
12. E. M. Bohn et al., "Reactivity Worth Measurements of a Simulated B_4C Control Rod Assembly in ZPR-6 Assembly 7, ANL-7910, pp. 135-141, Argonne National Laboratory (1972).
13. M. M. Bretscher and J. A. Morman, "Integral Alpha and Point Conversion Ratio Measurements in Advanced Fuels Critical Assemblies," to be published in Trans. Am. Nucl. Soc. 28,
14. S. G. Carpenter et al., "Measurement and Analysis of the Breeding Ratio in ZPPR Assembly 4 Phase I," Trans. Am. Nucl. Soc., 22, 693 (1975).